Research Article

Restoration and modification of magnetosome biosynthesis by internal gene acquisition in a magnetotactic bacterium

Atsushi Arakaki[1*], Mayu Goto[1], Mina Maruyama[1], Takuto Yoda[1], Masayoshi Tanaka[2], Ayana Yamagishi[1], Yasuo Yoshikuni[3], and Tadashi Matsunaga[1,4]

[1]Division of Biotechnology and Life Science, Institute of Engineering, Tokyo University of Agriculture and Technology, 2-24-16 Naka-cho, Koganei, Tokyo 184-8588, Japan
[2]Department of Chemical Science and Engineering, Tokyo Institute of Technology, 2-12-1 O-okayama, Meguro-ku, Tokyo 152-8550, Japan
[3]DNA Synthesis Science Program, The U.S. Department of Energy Joint Genome Institute, Lawrence Berkeley National Laboratory, Berkeley, CA94720, U.S.A.
[4]Japan Agency for Marine-Earth Science and Technology (JAMSTEC), 2-15, Natsushima-cho, Yokosuka, Kanagawa 237-0061, Japan

Correspondence: Atsushi Arakaki, Division of Biotechnology and Life Science, Institute of Engineering, Tokyo University of Agriculture and Technology, 2-24-16 Naka-cho, Koganei, Tokyo 184-8588, Japan. **E-mail:** arakakia@cc.tuat.ac.jp

Keywords: magnetotactic bacteria, genetic engineering, chromosomal integration, biomineralization, bioproduction

Abbreviations: ***M. magneticum* AMB-1**, *Magnetospirillum magneticum* AMB-1; **MAI**, magnetosome island; **MSGM**, magnetic spirillum growth medium; **NdB**, neodymium-boron; **TEM**, Transmission electron microscopy

Abstract

Integration of a large-sized DNA fragment into a chromosome is an important strategy for characterization of cellular functions in microorganisms. Magnetotactic bacteria synthesize intracellular organelles comprised of membrane-bound single crystalline magnetite, also referred to as magnetosomes. Magnetosomes have gained interest in both scientific and engineering sectors as they can be utilized as a material for biomedical and nanotechnological applications. Although genetic engineering of magnetosome biosynthesis mechanism has been investigated, the current method requires cumbersome gene preparation processes. Here, we showed the chromosomal integration of a plasmid containing ~27 magnetosome genes (~26 kbp region) in a non-magnetic mutant of *Magnetospirillum magneticum* AMB-1 using a broad-host-range plasmid. The genome sequencing of gene-complemented strains revealed the chromosomal integration of the plasmid with magnetosome genes at a specific site, most likely by catalysis of an endogenous transposase. Magnetosome production was successfully enhanced by integrating a variation of magnetosome gene operons in the chromosome. This chromosomal integration mechanism will allow us to design functional magnetosomes *de novo* and *M. magneticum* AMB-1 may be used as a chassis for the designed magnetosome production.

1 Introduction

Magnetotactic bacteria synthesize magnetic nanoparticles consisting of single crystalline magnetite (Fe_3O_4). The bacterial cells utilize chains of these magnetite particles as a compass to find preferential habitats in aquatic environments [1]. A magnetotactic bacterial strain, *Magnetospirillum magneticum* AMB-1, synthesizes approximately 20 cuboctahedral magnetite particles per cell with a mean diameter of 40 nm [2, 3]. The particles are formed within a subcellular organelle specialized for the synthesis of magnetite crystal, the magnetosome. The intracellular magnetites are individually covered with a biological membrane and show high dispersion in aqueous solutions when they are extracted from the bacterial cell [4]. In addition, the organic membrane is used as a surface to display functional molecules [5]. Magnetosomes are thus attractive for use in various biotechnological applications, such as immunoassays, cell separation, and drug-target screening [6].

The overall formation mechanism of magnetosomes was elucidated through a wide variety of analytical approaches, including genomics [7-9], proteomics [10, 11], gene mutagenesis [12, 13], and microscopy [14, 15]. The mechanism is comprised of multiple sequential biological events involving vesicle formation, iron uptake, and magnetite crystallization [6, 16]. The protein components involved in each process are localized to the surface of magnetosomes at appropriate times in a stepwise manner during magnetosome development [12, 17]. Genomic analyses of several magnetotactic bacteria revealed the existence of a common chromosomal region that encodes proteins that play a main role in magnetosome formation [8, 9]. This chromosomal region contains a genomic island-like structure, as it contains repetitive sequences at both ends, and is specifically referred to as a magnetosome island (MAI) [18]. The MAI of *M. magneticum* AMB-1 is approximately 98 kbp, encoding 99 genes [7]. *M. magneticum* AMB-1 spontaneously loses its MAI from the chromosome and generates a non-magnetic mutant (ΔMAI), indicating that this gene region is crucial for magnetosome formation [19]. In the MAI,

the genes are arranged in several operons that regulate magnetosome formation. The *mamAB* operon contains genes for vesicle formation, vesicle alignment, iron transport, and crystal formation [12, 20-22]. This was shown to be essential for magnetosome formation in both *M. magneticum* AMB-1 and *M. gryphiswaldense* MSR-1 by gene-deletion mutagenesis. Both *mamGFDC* and *mms6* operons encode proteins for magnetite crystal growth involving size and shape controls [13, 23-25].

In combination with an understanding of magnetosome formation mechanisms, genetic engineering approaches aiming to create new magnetosome-producing microorganisms have been investigated [16]. The magnetosome-forming ability of *M. gryphiswaldense* MSR-1 was successfully transferred into the non-magnetic photosynthetic bacterium, *Rhodospirillum rubrum*, by integrating a partial MAI region of approximately 26 kbp into the chromosome [26]. Random chromosomal insertion via transposition using MycoMar transposable elements was employed to retain this large DNA fragment in the chromosome. The same methodology has been used in *M. gryphiswaldense* MSR-1, where magnetosome numbers were enhanced and the magnetite crystal size was increased by multiplying the copy number of major MAI operons (*mms6*, *mamGFDC*, *mamAB*, and *mamXY* operons) [27]. Despite successful genetic modifications of magnetosome synthesis in these studies, some issues stand out, which need to be addressed for further engineering. First, the current method is cumbersome as it uses exogenous transposable elements in a narrow-host-range plasmid, whose preparation requires multiple cloning processes and specialized bacterial strains [26]. Second, the attempt to use a replicable multi-copy plasmid in *M. gryphiswaldense* MSR-1 failed. The plasmid harboring *mamAB* operon is unstable in the cells and spontaneous deletions and rearrangements in plasmids have been reported [27]. Thus, with specialized and tailored designs of gene sets, and increased sizes of DNA fragments to be introduced in the organisms, the development of alternative efficient and convenient genetic strategies is needed.

Here, we showed the introduction of 27 genes related to magnetosome biosynthesis into a ΔMAI of *M. magneticum* AMB-1 to restore the magnetosome-forming ability of the cells. A broad-host-range plasmid, pRK415 [28], a derivative of the RK2 replicon, was used for the gene introduction. This examination coincidentally identified a new gene insertion mechanism enabling the integration of large DNA fragments into chromosomes without the aid of a foreign transposable element. The gene integration was specific, reproducible, and applied to modify magnetosome biosynthesis in *M. magneticum* AMB-1 cells.

2 Materials and methods

2.1 Strains and growth conditions

Strains, plasmids, and primers are described in detail in Supplementary Table 1. *Escherichia coli* (*E. coli*) strains, TOP10 (Invitrogen), and EPI300 (Epicentre, Wisconsin, U.S.A.) were used for gene cloning. *E. coli* cells were cultured in Luria Broth (LB) medium at 37°C, after the addition of appropriate antibiotics. For conjugation experiments, *E. coli* S17-1 (ATCC47055) was used as a donor and cultivated. *M. magneticum* AMB-1 (ATCC700264) was anaerobically grown in a 25 ml glass vial or a 10 l flask using magnetic spirillum growth medium (MSGM) at 28°C. Colonies of *M. magneticum* AMB-1 were obtained on an MSGM plate that was incubated microaerobically at 28°C.

ΔMAI was obtained as described previously [19]. Briefly, cultures of *M. magneticum* AMB-1 wild type strain were magnetically separated with a neodymium-boron (NdB) magnet (diameter, 15 mm; height, 1 cm) closely attached to the side of a 25 ml vial containing 10 ml of cell culture. The cells that were not collected with the magnet were sampled from the vial and plated on solid MSGM media. The obtained white colonies were then cultivated in liquid culture. MAI deletion was confirmed by genome sequencing, and the strain was utilized as a ΔMAI.

2.2 Plasmid construction

The *mamGFDC*, *mms6*, *mamAB*, and *mamXY* gene operons from *M. magneticum* AMB-1 were cloned into pRK415 by Gibson assembly [29]. *Swa*I restriction sites were added to both ends of the *mamGFDC*, *mms6*, *mamAB*, and *mamXY* gene operons by PCR, since no restriction enzyme site is present in these operons. The PCR amplified fragments were used for assembly. pRK-A containing the *mamAB* gene operon, pRK-G6 containing the *mamGFDC* and *mms6* gene operons, and pRK-G6A containing the *mamGFDC*, *mms6*, and *mamAB* gene operons, were constructed.

2.3 Gene introduction into ΔMAI

The constructed plasmids harboring MAI genes were introduced into the ΔMAI by conjugation using *E. coli* S17-1 as the donor strain. Conjugation was conducted on solid MSGM media for 6 h. After conjugation, cells were cultured in 25 ml vials containing 10 ml MSGM medium with tetracycline (10 μg/ml). After 5 days of cultivation, cells were plated on solid medium with tetracycline (10 μg/ml) and cultured anaerobically using an anaerobic bag (Anaerocult®P, Merck KGaA, Darmstadt, Germany). The remaining cells in the vials were separated to place a NdB magnet on the side of glass vial. The supernatant was discarded, and the cell pellet was resuspended with 10 ml of fresh medium in the vial. The magnetically separated cells were cultured for 5 days. Using the same procedure, cells were repeatedly cultured over five passages. The magnetosome formation ability of the cells was analyzed by observing their magnetic response under an optical microscope and the presence of magnetosomes under a transmission electron microscope in each passage number. Plasmids were extracted from 200 ml magnetotactic bacterial cultures. The cells showing magnetic response were confirmed microscopically before plasmid extraction.

2.4 Transmission electron microscopy (TEM)

TEM analysis was performed using JEM1200EX (JEOL Ltd., Tokyo, Japan) at 100 or 120 kV. At least 200 crystals from at least 10 cells of each strain were analyzed, and the crystal size (average major axis and minor axis) was evaluated. The cells were randomly selected and only crystals with sizes ≥ 5 nm were measured in this study.

2.5 Genome and DNA sequencing

Plasmid constructions and genome sequences were analyzed using a Hiseq 2000 sequencer (Illumina, Inc., San Diego, CA, USA). Gaps between contigs were sequenced by a 3730xl DNA Analyzer (Applied Biosystems, Waltham, MI, USA). The contigs were compared with the genome data of AMB-1 (AP007255) and pRK415 (EF437940) from NCBI by BLAST search.

2.6 SDS-PAGE

Magnetite crystals were extracted from 10 l of culture (wild type and ΔMAI-pRK-G6A) and washed 5 times with 10 mM HEPES (pH 7.0). The other cell fractions were prepared as described previously [24]. To isolate the proteins, magnetite crystals were treated three times with 200 μl of 1% (w/v) SDS in a 100°C water bath for 30 min. Electrophoretic separation of proteins was carried out on a 20% acrylamide gel. Proteins (40 μg) were loaded into each 7 mm well of the gel in sample buffer and separated at 40 mA. The gel was stained with Bio-Safe Coomassie G-250 (Bio-Rad, Tokyo, Japan).

2.7 Cell growth and iron measurements

Cell concentration was measured by hemocytometry. The iron concentration from cell-free culture supernatants was determined using an inductively coupled plasma atomic emission spectrometer (ICPE-9000, Shimadzu, Kyoto, Japan).

3 Results and discussion

3.1 Introduction of a plasmid harboring magnetosome genes into ΔMAI

A ΔMAI of *M. magneticum* AMB-1 (Supplementary Figure 1) was generated by a method described previously [19]. Deletion of the entire 98 kbp region of the MAI at position nt 997403–1095894 on the chromosome (Figure 1A) was confirmed by PCR and genome sequencing. The results suggested that the spontaneous gene deletion of the MAI at this chromosome site is reproducible and occurs frequently in this organism.

To reconstruct the magnetosome biosynthesis function in ΔMAI, the *mms6*, *mamGFDC*, and *mamAB* operons were cloned into a broad-host-range plasmid, pRK415, which is replicable in *M. magneticum* AMB-1 [30]. The derivative plasmids were designated as pRK-A (*mamAB* operon), pRK-G6 (*mms6* and *mamGFDC* operons), and pRK-G6A (*mms6*, *mamGFDC*, and *mamAB* operons), respectively (Figure 1B–1D). The plasmids were then introduced into ΔMAI by conjugal gene transfer using *E. coli* S17-1. After plating the cells on solid media, colonies exhibiting antibiotic resistance were obtained for pRK-G6, pRK-A, and pRK-G6A with a transformation efficiency of 10^{-2}–10^{-5}; this is comparable to the efficiency in pRK415 [30]. However, the obtained cells produced no magnetosomes and showed non-magnetotactic behavior. The cells contained plasmids, although the size of the extracted plasmids and band patterns after restriction enzyme treatment were not consistent with those of the original plasmid (Supplementary Figure 2). Sequencing of the plasmids revealed spontaneous deletions in the region of *mamAB* genes and promoter, as reported previously [27]. Because involvement of endogenous *recA* in the frequent mutations of the MAI region is reported in *M. gryphiswaldense* MSR-1 [31], the same experiment was conducted to use ΔMAI *recA*$^{-}$ of *M. magneticum* AMB-1 (constructed in this study). However, gene deletions and rearrangements were also determined in this strain (data not shown), suggesting that the mutations were caused by other recombination

mechanisms. The copy number of the vector pRK415 is 3 ± 1 copies/cell in AMB-1 [30], and thus expression levels of *mamAB* genes in the transformants can be higher than those in the wild type. The observation of this study suggests that the *mamAB* region in multi-copy plasmids imposes a significant burden on the cells, and inhibits their growth. On the other hand, the compensatory mutations in the plasmid may reduce the cost of carriage [32]. Cells harboring mutated plasmids with less or no expression of the *mamAB* genes may be preferentially grown in the media. In contrast, pRK-G6, which only harbors genes that have a role in crystal formation, was found to be stably maintained as the original construct in ΔMAI. Although the cells did not produce magnetite, the result was consistent with previous studies [12].

Then, we changed the strategy to isolate gene-complemented cells. After conjugation of the pRK-G6A plasmid, cells were directly transferred to liquid medium and cultured. After 72 h of cultivation for the first passage, approximately 90% of the cells showed a magnetic response, suggesting recovery of magnetosome formation ability. The cells were also collectable by a magnet (Supplementary Figure 3). Under TEM, formation of electron-dense spherical particles in the cells was observed (Figure 2A, and 2E). The average particle number was 87.3 ± 33.2 particles/cell (average ± S.D.), which is approximately 4 times larger than that in the wild type strain. Magnetosomes were distributed as several chains or as a bundle of chains in the cell. The average particle size was 13.1 ± 6.3 nm (average ± S.D.), which is smaller than those of the wild type strain (approximately 38 nm). However, the introduced pRK-G6A plasmid was not confirmed by plasmid extraction. In addition, the cells became non-magnetic when inoculated on solid media for isolation as a single clone. The non-magnetic cells contained a mutated plasmid similar to the one shown in Supplementary Figure 2. Therefore, we repeatedly cultured the magnetic cells in liquid media, and tried to isolate the magnetic cells on solid media in each passage number (Figure 2B–2D, and 2F–2H). After the third passage, some cells contained magnetosomes with a single chain-like structure. After the fifth passage, a gene-complemented

strain producing magnetosomes was successfully isolated as a single clone on the solid medium, and this strain was named as ΔMAI-pRK-G6A.

TEM analysis of ΔMAI-pRK-G6A showed that the average particle number and size of magnetosomes were 29.9 ± 15.4 particles/cell and 15.7 ± 2.9 nm, respectively (Table 1). The presence of membranous structures surrounding magnetite crystals was also confirmed by thin-sectioned samples of ΔMAI-pRK-G6A (Figure 3A). For the determination of magnetosome protein expression, proteins extracted from the magnetosome membrane were analyzed by SDS-PAGE. The magnetosome protein from the ΔMAI-pRK-G6A strain showed a similar band pattern to that of the wild type strain (Figure 3B). The two bands observed at approximately 24 kDa and 13 kDa in ΔMAI-pRK-G6A were analyzed by mass spectrometry. As expected, magnetosome proteins such as MamA, Mms13 (MamC), and Mms6 were detected from these bands (Supplementary Table 2). Some minor differences in the protein bands between the two strains would be mainly due to genetic differences, because the ΔMAI-pRK-G6A strain contains partial magnetosome genes. Expression of introduced magnetosome genes in ΔMAI-pRK-G6A was also analyzed by reverse transcription-PCR. The expression of genes in *mamGFDC, mms6,* and *mamAB* operons was detected in both wild type and ΔMAI-pRK-G6A strains for all tested regions, but they were not detected in the ΔMAI strain (Supplementary Figure 4). Negative control experiments performed without the reverse transcriptase enzyme revealed the absence of DNA from the RNA samples. These results indicated that ΔMAI-pRK-G6A cells express the genes for the *mamGFDC-mms6-mamAB* operons.

3.2 Identification of magnetosome genes in the chromosome of a gene-complemented strain

Plasmid extraction was reexamined to show the presence of pRK-G6A in gene-complemented cells. However, no band corresponding to pRK-G6A was determined by gel electrophoresis (Supplementary Figure 5, lane 1). On the other hand, a band corresponding to pRK415 was

clearly detected when pRK415 was transformed into wild type or ΔMAI strains (Supplementary Figure 5, lane 4). This indicates that pRK-G6A was no longer present in ΔMAI-pRK-G6A as a plasmid. Insertion of the magnetosome genes into the chromosomal DNA of ΔMAI was considered.

To clarify the presence of introduced MAI genes in gene-complemented cells, genome sequencing was conducted using a HiSeq2000 sequencer. Four ΔMAI-pRK-G6A clones obtained from 3 independent experiments (clone no. 1–4) were analyzed as representative samples of this investigation. Clones no. 1 and 2 were obtained in the same experiment. The contigs listed in Supplementary Table 3 were constructed by aligning the read sequences. Contigs containing matches with pRK415 longer than 12 bp were extracted to avoid coincidental matching with the AMB-1 genome. Three to four contigs-containing sequences corresponding to pRK415 were found in all analyzed clones (Supplementary Table 3). Gaps between contigs for each clone were amplified by PCR and the obtained fragments were sequenced. The aligned sequences completely matched with the sequence of pRK-G6A. Contigs containing sequences of both pRK-G6A and the chromosome of *M. magneticum* AMB-1 were also found. These results indicated that the pRK-G6A plasmid was integrated into the chromosome of ΔMAI.

Based on the obtained sequences from the 4 clones, the integration site of the plasmid in the genome of ΔMAI was determined (Figure 4A). The plasmid integration site was different from the original locus of MAI in wild type strain. The pRK-G6A plasmid was placed between two genes, amb3760 and amb3761. Six genes encoding transposition proteins (amb3758, amb3759, amb3760, amb3763, amb3764, and amb3765) were co-located in the flanking region. The amb3758, and both amb3759 and amb3764 genes are homologs of endonuclease (*tnsB*) and integrase (*tnsA*) of the Tn7 element, respectively [33]. Both amb3760 and amb3765 encode a homolog of the TniQ protein, which is a target selector of the Tn5090/Tn5053 element [34]. Interestingly, the integration site of pRK-G6A in the chromosome was the same for the 4 clones.

A set of inverted repeat (IR) sequences with 8 bp length was commonly found (Figure 4A). In addition, 5 bp repetitive sequences were placed right next to the 8 bp IR sequences. The 5 bp sequences originated from the sequence of pRK415, and these sequences were likely duplicated during chromosomal integration of pRK-G6A. Furthermore, the direction of pRK-G6A integration in the chromosome for clone nos. 1 and 2 was opposite to that for clone nos. 3 and 4, suggesting that the direction is random. For clones no. 1, 2, and 4, pRK415-G6A was disconnected near the *oriV* of this plasmid (60 bp apart from *oriV*) (Figure 4B). The target site of gene insertion for clone no. 3 was different from the other three clones, and was 14 bp apart from that of the other clones. Among the 4 clones, the 4 bp sequence (GAAG) in ΔMAI was replaced with the entire sequence of pRK415-G6A.

The repetitive inverse repeats sequences of 8 bp in the chromosome at the plasmid insertion site, and the formation of 5 bp repeat sequences in the same direction were commonly found in all clones. Among various gene acquisition mechanisms, the characters found in the genome sequence coincide with those of transposon and insertion sequence elements [32, 35]. Because pRK415 does not contain an internal transposase, it is likely derived from the chromosome of the host genome. Tn7 and Tn5090/Tn5053 contribute to the formation of genomic islands [34]. The gene sets found in the flanking sequence of gene insertion sites are most likely involved in the observed plasmid integration of this study. Interestingly, direct repeats are formed by the side of the plasmid (Figure 4B). Based on the transposition mechanism used by the transposons, the gene integration mechanism observed in this study can be explained through the integration of AMB-1 chromosome into the plasmid.

Genomic integration of plasmids is reported in many different bacterial species to date [36, 37], and is typically seen in plasmids harboring pathogenic or drug resistance genes. Gene acquisition is important for these organisms as a survival strategy in their environment. Similarly, magnetotactic bacteria are suggested to use magnetosomes to find low oxygen

atmospheres for their survival [1]. Spontaneous deletions of the MAI region and an increase in its frequency due to exposure to oxygen or high iron concentrations are also reported [18, 19]. Moreover, genome analyses revealed the presence of a large number of IS elements, phage-related genes, and non-uniform distribution of GC contents, suggesting that the occurrence of genomic rearrangement events includes external DNA integration and intra-molecular recombination [7, 8, 38]. Genetic plasticity is thus a common characteristic in this group of organisms. The observed chromosomal integration of plasmids in this study can be part of a mechanism where the organism acquired foreign DNA including MAI genes.

3.3 Engineering of magnetosome biosynthesis using the internal gene acquisition mechanism

The identified gene integration mechanism was applied to modify the magnetosome biosynthesis function in *M. magneticum* AMB-1 (Figure 5). Using the same procedure with ΔMAI-pRK-G6A, ΔMAI-pRK-A was successfully obtained as an isolate (Figures 5B and 5F). ΔMAI-pRK-A contains only *mamAB* operon, which has been shown to be essential for magnetosome biosynthesis in *Magnetosprillum spp*. by gene deletion mutagenesis [12]. On the contrary, inserting only *mamAB* operon in *R. rubrum* does not allow the cells to form magnetosomes [26]. The result of this study indicates for the first time that the *mamAB* operon alone can restore the magnetosome formation ability in *Magnetosprillum spp*. As expected, the average particle number and size in ΔMAI-pRK-A were smaller relative to those in ΔMAI-pRK-G6A (Table 1). The results also indicate that additional introduction of *mms6* and *mamGFDC* operons, which play key roles in magnetite crystal formation [13], can increase particle number and size. This is consistent with the previous knowledge regarding *M. gryphiswaldense* MSR-1 [27].

The internal gene integration mechanism of *M. magneticum* AMB-1 was further investigated to enhance magnetosome productivity in bacterial cells. Doubling of *mms6*, *mamGFDC*, and

mamAB operons in a chromosome was conducted by introducing pRK-G6A into the wild type strain. The established strain, WT-pRK-G6A, successfully synthesized more magnetosomes than those synthesized by the wild type strain (Figures 5D and 5H). The average size and number of magnetosomes in WT-pRK-G6A strain were 33.8 ± 13.7 nm and 44.4 ± 9.1 particles/cell, respectively (Table 1). The result indicated that introducing an additional set of the magnetosome genes enhances the number of magnetosomes in the cell, as also reported previously in another strain using a different method [27]. WT-pRK-G6A genome sequencing revealed the presence of original MAI with pRK-G6A plasmid integration into the wild type chromosome. The chromosomal integration site and direction in WT-pRK-G6A were identical to those in ΔMAI-pRK-G6A clone nos. 1 and 2 (Figure 4A).

The cell growth, iron uptake, and magnetosome production of WT-pRK-G6A strain were further characterized and compared with those of the wild type and ΔMAI strains. Cells were inoculated in liquid media containing approximately 32 μM iron. After cultivating for 120 h, no significant difference in cell concentration was observed among the three strains (Figure 6A) and the iron concentration in media decreased to approximately 22–23 μM (Figure 6B). The result indicates that iron uptake ability of the three strains is comparable. Finally, magnetosome production was evaluated by cultivating WT-pRK-G6A cells in a large scale (10 l) fed-batch culture and the yield was found to be 8.6 ± 2.0 mg/l, which is higher than that of the wild type strain (7.5 mg/l) [39].

Based on the cell concentration and decreased iron amount in the media, the mean cellular iron content per cell was estimated. The average cell number and iron consumption at 96 h, 102 h, and 120 h as shown in Figure 6 were used for this estimation. The iron content per cell was calculated as 4.9 ± 0.6 fg/cell, 4.7 ± 0.4 fg/cell, and 5.4 ± 0.2 fg/cell for wild type, WT-pRK-G6A, and ΔMAI strains, respectively (Table 2). The iron content in magnetite per cell was also calculated based on the average magnetosome size as shown in Table 1. The iron content in

magnetite was 2.4 fg/cell and 3.4 fg/cell for the wild type and WT-pRK-G6A strains, respectively. This estimation clearly indicates that *mamGFDC*, *mms6*, and *mamAB* operon introduction facilitates magnetite biomineralization, but not iron uptake into the cell. The conversion of cellular iron ion to mineralized magnetite form was approximately 49% and 72% in the wild type and WT-pRK-G6A strains, respectively.

This study indicated the presence of an unidentified internal chromosomal gene integration mechanism in magnetotactic bacteria. A simple and reproducible gene introduction strategy enabling the modification of magnetosome biosynthesis based on gene integration was shown. This gene integration mechanism may be used as an alternative method to modify and optimize the magnetosome formation ability of cells for the mass production of functional magnetosomes. In addition, our results also suggest that *M. magneticum* AMB-1 cell is a useful genetic tool to analyze the functions of large-sized gene operons from other organisms. The gene integration mechanism will allow us to analyze uncharacterized foreign genes including magnetosomal genes from uncultivated magnetotactic bacterium. For further enhancement of magnetosome biosynthesis in *M. magneticum* AMB-1, the introduction of both magnetosome and iron transporter genes is required.

4 Concluding remarks

In this study, a pRK415 plasmid harboring a large gene region involved in magnetosome formation was inserted into *M. magneticum* AMB-1 ΔMAI chromosome, which successfully restored the magnetosome formation ability. The chromosomal gene integration only occurred when pRK415 harbored the *mamAB* gene operon. The gene-integrated region of the complemented strain revealed the formation of unique 5 bp and 8 bp repeat sequences, suggesting that chromosomal integration involves endogenous transposon-like gene insertion mechanisms. The gene-complemented strains showed the restoration of magnetosome formation

ability, depending on the integrated gene set. The magnetosome production was enhanced by the insertion of magnetosome gene operons in the wild type strain.

Acknowledgements

The authors thank Naoki Aoyagi and Satoshi Murata (Tokyo University of Agriculture and Technology) for their assistance in MS analysis. A.A. and T.M. would like to acknowledge financial support from a Grant-in-Aid for Scientific Research (A) (no. 16H02421) from the Japan Society for the Promotion of Science (JSPS). A.A. also would like to acknowledge financial support from a Grant-in-Aid for Scientific Research (B) (no. 18H01794) from the JSPS. Y.Y would like to thank to the support from the U.S. Department of Energy Joint Genome Institute, a DOE Office of Science User Facility, is supported under Contract No. DE-AC02-05CH11231. A.A. and Y.Y. also would like to thank to the support from Institute of Global Innovation Research (GIR) at TUAT.

Conflict of interest

The authors declare no conflict of interest directly relevant to the content of this article.

5 References

[1] Blakemore, R., Magnetotactic bacteria. *Science* 1975, *190*, 377-379.

[2] Tanaka, M., Mazuyama, E., Arakaki, A., Matsunaga, T., MMS6 protein regulates crystal morphology during nano-sized magnetite biomineralization *in vivo*. *J Biol Chem* 2011, *286*, 6386-6392.

[3] Matsunaga, T., Sakaguchi, T., Tadokoro, F., Magnetite formation by a magnetic bacterium capable of growing aerobically. *Appl Microbiol Biotechnol* 1991, *35*, 651-655.

[4] Nakamura, N., Hashimoto, K., Matsunaga, T., Immunoassay method for the determination of immunoglobulin-G using bacterial magnetic particles. *Anal Chem* 1991, *63*, 268-272.

[5] Yoshino, T., Takahashi, M., Takeyama, H., Okamura, Y.*, et al.*, Assembly of G protein-coupled receptors onto nanosized bacterial magnetic particles using Mms16 as an anchor molecule. *Appl Environ Microbiol* 2004, *70*, 2880-2885.

[6] Arakaki, A., Nakazawa, H., Nemoto, M., Mori, T., Matsunaga, T., Formation of magnetite by bacteria and its application. *J R Soc Interface* 2008, *5*, 977-999.

[7] Matsunaga, T., Okamura, Y., Fukuda, Y., Wahyudi, A. T.*, et al.*, Complete genome sequence of the facultative anaerobic magnetotactic bacterium *Magnetospirillum* sp. strain AMB-1. *DNA Res* 2005, *12*, 157-166.

[8] Nakazawa, H., Arakaki, A., Narita-Yamada, S., Yashiro, I.*, et al.*, Whole genome sequence of *Desulfovibrio magneticus* strain RS-1 revealed common gene clusters in magnetotactic bacteria. *Genome Res* 2009, *19*, 1801-1808.

[9] Jogler, C., Kube, M., Schübbe, S., Ullrich, S.*, et al.*, Comparative analysis of magnetosome gene clusters in magnetotactic bacteria provides further evidence for horizontal gene transfer. *Environ Microbiol* 2009, *11*, 1267-1277.

[10] Tanaka, M., Okamura, Y., Arakaki, A., Tanaka, T.*, et al.*, Origin of magnetosome membrane: proteomic analysis of magnetosome membrane and comparison with cytoplasmic membrane. *Proteomics* 2006, *6*, 5234-5247.

[11] Grünberg, K., Müller, E. C., Otto, A., Reszka, R.*, et al.*, Biochemical and proteomic analysis of the magnetosome membrane in *Magnetospirillum gryphiswaldense*. *Appl Environ Microbiol* 2004, *70*, 1040-1050.

[12] Murat, D., Quinlan, A., Vali, H., Komeili, A., Comprehensive genetic dissection of the magnetosome gene island reveals the step-wise assembly of a prokaryotic organelle. *Proc Natl Acad Sci U S A* 2010, *107*, 5593-5598.

[13] Arakaki, A., Yamagishi, A., Fukuyo, A., Tanaka, M., Matsunaga, T., Co-ordinated functions of Mms proteins define the surface structure of cubo-octahedral magnetite crystals in magnetotactic bacteria. *Mol Microbiol* 2014, *93*, 554-567.

[14] Taoka, A., Kiyokawa, A., Uesugi, C., Kikuchi, Y., *et al.*, Tethered magnets are the key to magnetotaxis: direct observations of *Magnetospirillum magneticum* AMB-1 show that MamK distributes magnetosome organelles equally to daughter cells. *Mbio* 2017, *8*, e00679-17.

[15] Gorby, Y. A., Beveridge, T. J., Blakemore, R. P., Characterization of the bacterial magnetosome membrane. *J Bacteriol* 1988, *170*, 834-841.

[16] Uebe, R., Schüler, D., Magnetosome biogenesis in magnetotactic bacteria. *Nat Rev Microbiol* 2016, *14*, 621-637.

[17] Arakaki, A., Kikuchi, D., Tanaka, M., Yamagishi, A., *et al.*, Comparative subcellular localization analysis of magnetosome proteins reveals a unique localization behavior of Mms6 protein onto magnetite crystals. *J Bacteriol* 2016, *198*, 2794-2802.

[18] Ullrich, S., Kube, M., Schübbe, S., Reinhardt, R., Schüler, D., A hypervariable 130-kilobase genomic region of *Magnetospirillum gryphiswaldense* comprises a magnetosome island which undergoes frequent rearrangements during stationary growth. *J Bacteriol* 2005, *187*, 7176-7184.

[19] Fukuda, Y., Okamura, Y., Takeyama, H., Matsunaga, T., Dynamic analysis of a genomic island in *Magnetospirillum* sp. strain AMB-1 reveals how magnetosome synthesis developed. *FEBS Lett* 2006, *580*, 801-812.

[20] Komeili, A., Li, Z., Newman, D. K., Jensen, G. J., Magnetosomes are cell membrane invaginations organized by the actin-like protein MamK. *Science* 2006, *311*, 242-245.

[21] Uebe, R., Junge, K., Henn, V., Poxleitner, G., *et al.*, The cation diffusion facilitator proteins MamB and MamM of *Magnetospirillum gryphiswaldense* have distinct and complex functions, and are involved in magnetite biomineralization and magnetosome membrane assembly. *Mol Microbiol* 2011, *82*, 818-835.

[22] Siponen, M. I., Legrand, P., Widdrat, M., Jones, S. R., *et al.*, Structural insight into magnetochrome-mediated magnetite biomineralization. *Nature* 2013, *502*, 681-684.

[23] Murat, D., Falahati, V., Bertinetti, L., Csencsits, R., *et al.*, The magnetosome membrane protein, MmsF, is a major regulator of magnetite biomineralization in *Magnetospirillum magneticum* AMB-1. *Mol Microbiol* 2012, *85*, 684-699.

[24] Arakaki, A., Webb, J., Matsunaga, T., A novel protein tightly bound to bacterial magnetic particles in *Magnetospirillum magneticum* strain AMB-1. *J Biol Chem* 2003, *278*, 8745-8750.

[25] Scheffel, A., Gärdes, A., Grünberg, K., Wanner, G., Schüler, D., The major magnetosome proteins MamGFDC are not essential for magnetite biomineralization in *Magnetospirillum gryphiswaldense* but regulate the size of magnetosome crystals. *J Bacteriol* 2008, *190*, 377-386.

[26] Kolinko, I., Lohsse, A., Borg, S., Raschdorf, O.*, et al.*, Biosynthesis of magnetic nanostructures in a foreign organism by transfer of bacterial magnetosome gene clusters. *Nat Nanotechnol* 2014, *9*, 193-197.

[27] Lohße, A., Kolinko, I., Raschdorf, O., Uebe, R.*, et al.*, Overproduction of magnetosomes by genomic amplification of biosynthesis-related gene clusters in a magnetotactic bacterium. *Appl Environ Microbiol* 2016, *82*, 3032-3041.

[28] Keen, N. T., Tamaki, S., Kobayashi, D., Trollinger, D., Improved broad-host-range plasmids for DNA cloning in gram-negative bacteria. *Gene* 1988, *70*, 191-197.

[29] Gibson, D. G., Young, L., Chuang, R. Y., Venter, J. C.*, et al.*, Enzymatic assembly of DNA molecules up to several hundred kilobases. *Nat Methods* 2009, *6*, 343-345.

[30] Matsunaga, T., Nakamura, C., Burgess, J. G., Sode, K., Gene-transfer in magnetic bacteria - transposon mutagenesis and cloning of genomic DNA fragments required for magnetosome synthesis. *J Bacteriol* 1992, *174*, 2748-2753.

[31] Kolinko, I., Jogler, C., Katzmann, E., Schüler, D., Frequent mutations within the genomic magnetosome island of *Magnetospirillum gryphiswaldense* are mediated by RecA. *J Bacteriol* 2011, *193*, 5328-5334.

[32] Porse, A., Schonning, K., Munck, C., Sommer, M. O. A., Survival and evolution of a large multidrug resistance plasmid in new clinical bacterial hosts. *Mol Biol Evol* 2016, *33*, 2860-2873.

[33] Parks, A. R., Peters, J. E., Tn7 elements: engendering diversity from chromosomes to episomes. *Plasmid* 2009, *61*, 1-14.

[34] Peters, J. E., Fricker, A. D., Kapili, B. J., Petassi, M. T., Heteromeric transposase elements: generators of genomic islands across diverse bacteria. *Mol Microbiol* 2014, *93*, 1084-1092.

[35] Bellanger, X., Payot, S., Leblond-Bourget, N., Guedon, G., Conjugative and mobilizable genomic islands in bacteria: evolution and diversity. *Fems Microbiol Rev* 2014, *38*, 720-760.

[36] Pilla, G., McVicker, G., Tang, C. M., Genetic plasticity of the *Shigella* virulence plasmid is mediated by intra- and inter-molecular events between insertion sequences. *PLoS Genet* 2017, *13*, e1007014.

[37] Modi, R. I., Castilla, L. H., Puskasrozsa, S., Helling, R. B., Adams, J., Genetic changes accompanying increased fitness in evolving populations of *Escherichia coli*. *Genetics* 1992, *130*, 241-249.

[38] Ji, B. Y., Zhang, S. D., Arnoux, P., Rouy, Z., *et al.*, Comparative genomic analysis provides insights into the evolution and niche adaptation of marine *Magnetospira* sp QH-2 strain. *Environ Microbiol* 2014, *16*, 525-544.

[39] Yang, C., Takeyama, H., Matsunaga, T., Iron feeding optimization and plasmid stability in production of recombinant bacterial magnetic particles by *Magnetospirillum magneticum* AMB-1 in fed-batch culture. *J Biosci Bioeng* 2001, *91*, 213-216.

Table 1. Summary of the number and size of magnetosomes formed within wild type, ΔMAI-pRK-A, ΔMAI-pRK-G6A, and WT-pRK-G6A strains

Strain	Particle number (particles/cell)	Particle size (nm)
Wild type	21.9 ± 3.5	38.2 ± 14.6
ΔMAI-pRK-A	19.5 ± 13.8	13.7 ± 5.9
ΔMAI-pRK-G6A	29.9 ± 15.4	15.7 ± 2.9
WT-pRK-G6A	44.4 ± 9.1	33.8 ± 13.7

Data is given as the mean ± standard deviation. Particle size is the average of major and minor axes. Cells and particles were randomly selected and only crystals with sizes ≥ 5 nm were measured. At least 200 particles from at least 10 cells were measured for each strain.

Table 2. Conversion rate of iron ions to bacterial magnetite particles in a cell

Strains	Iron amount in a single bacterial cell (fg/cell)	Iron amount in magnetite particles of a single bacterial cell (fg/cell)	Iron conversion rate for magnetic particles (%)
Wild type	4.9 ± 0.6	2.4	48.6 ± 5.8
WT-pRK-G6A	4.7 ± 0.4	3.4	72.3 ± 6.7
ΔMAI	5.4 ± 0.2	0	0

The mean iron amount in a single bacterial cell was calculated based on the average cell number and iron consumption at 96 h, 102 h, and 120 h as shown in Figure 6. The mean iron content in magnetite per bacterial cell was calculated based on the average magnetosome size as summarized in Table 1. Iron conversion rate for magnetic particles was calculated by dividing the iron amount in magnetite particles of a single bacterial cell by iron conversion rate for magnetic particles.

Figure legends

Figure 1. Gene organization of the MAI region of *M. magneticum* AMB-1 (A). Plasmid maps of pRK415 derivatives, pRK-A (B), pRK-G6 (C), and pRK-G6A (D).

Figure 2. Transmission electron micrographs of ΔMAI-pRK-G6A cells (A–D) and enlarged images of magnetosomes (E–H). Cells cultured in liquid media for 72 h after conjugation (A and E); cells in the first passage (B and F), the third passage (C and G), and the fifth passage (D and H) of cultivation.

Figure 3. Thin-section transmission electron micrograph of ΔMAI-pRK-G6A cells (A) and SDS-PAGE of the magnetosome protein fraction (B). Lane 1, magnetosome protein fraction from wild type; Lane 2, magnetosome protein fraction from ΔMAI-pRK-G6A. Arrows indicate bands subjected for LC-MS/MS analysis.

Figure 4. Molecular organization of the plasmid insertion region in ΔMAI-pRK-G6A clones (A). Three variants obtained from the genome sequences of 4 clones (clone no. 1–4) are presented. Grey arrows: inverted repeat (IR) and black arrows: direct repeat. Schematic of chromosomal integration of pRK-G6A (B). Highlighted in black: sequences of target sites for gene insertion. IRs from ΔMAI chromosome contact to the target sequences in pRK-G6A.

Figure 5. Transmission electron micrographs of wild type (A), ΔMAI-pRK-A (B), ΔMAI-pRK-G6A (C), and WT-pRK-G6A (D) strains. Enlarged images of magnetosomes for the wild type (E), ΔMAI-pRK-A (F), ΔMAI-pRK-G6A (G), and WT-pRK-G6A (H).

Figure 6. Growth curves (A) and time course of iron concentration in the media (B) of the wild type, ΔMAI, and WT-pRK-G6A. Each data point represents the mean (± S.D.) of three replicated vessels.

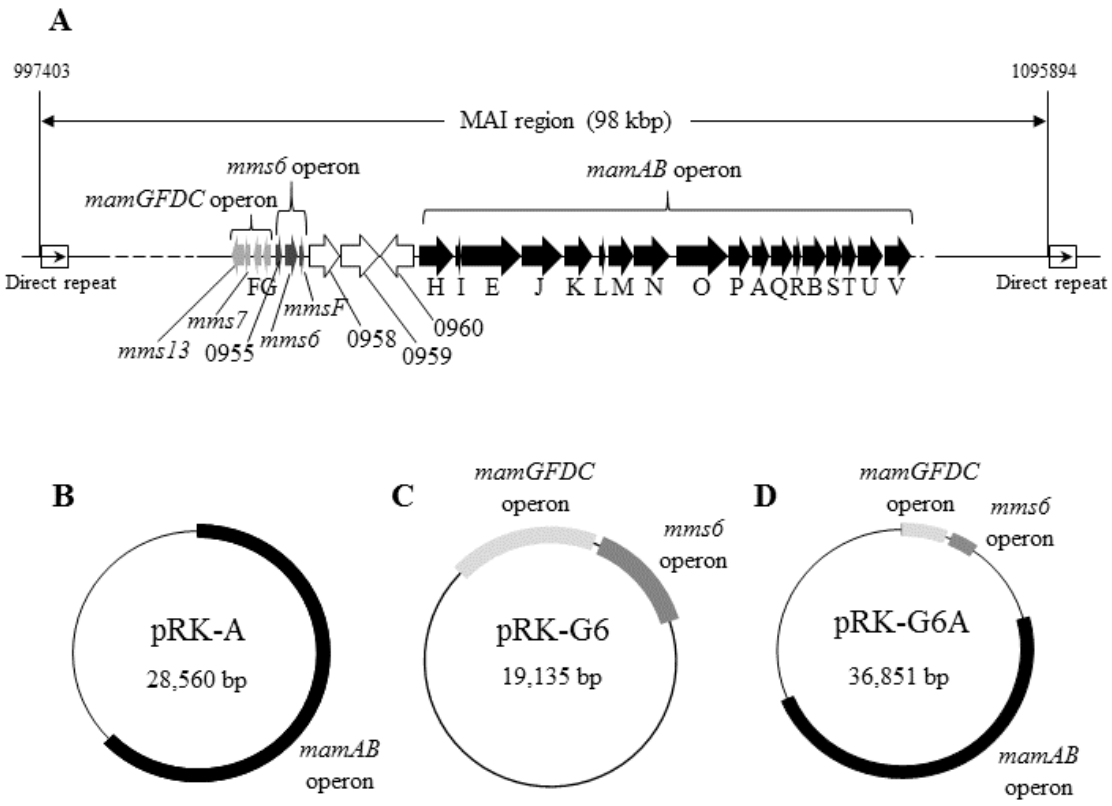
A
997403
1095894
MAI region (98 kbp)
mms6 operon
mamGFDC operon
mamAB operon
Direct repeat
FG
mms7
mms13
0955
mmsF
mms6
0958
0959
0960
H I E J K L M N O P A Q R B S T U V
Direct repeat
B
pRK-A
28,560 bp
mamAB
operon
C
mamGFDC
operon
mms6
operon
pRK-G6
19,135 bp
D
mamGFDC
operon
mms6
operon
pRK-G6A
36,851 bp
mamAB
operon

Fig. 1

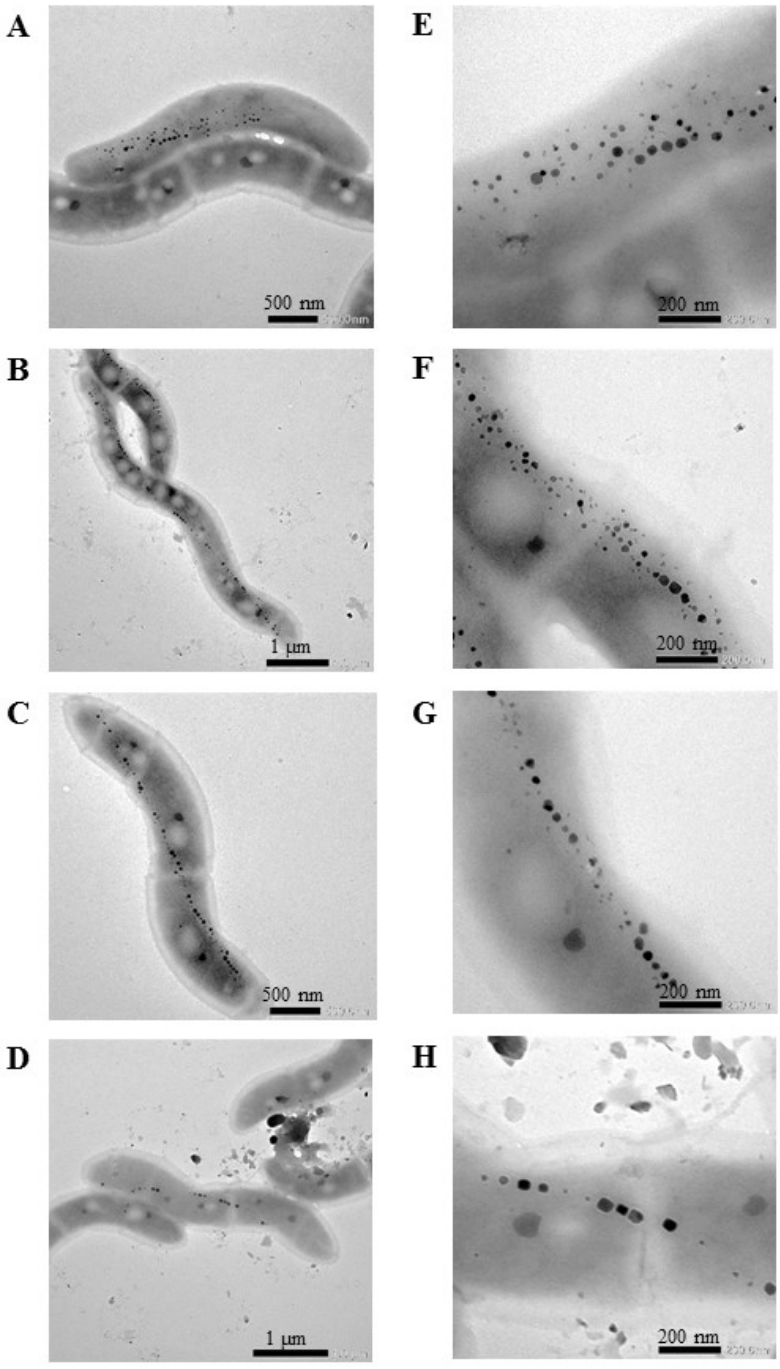

Fig. 2

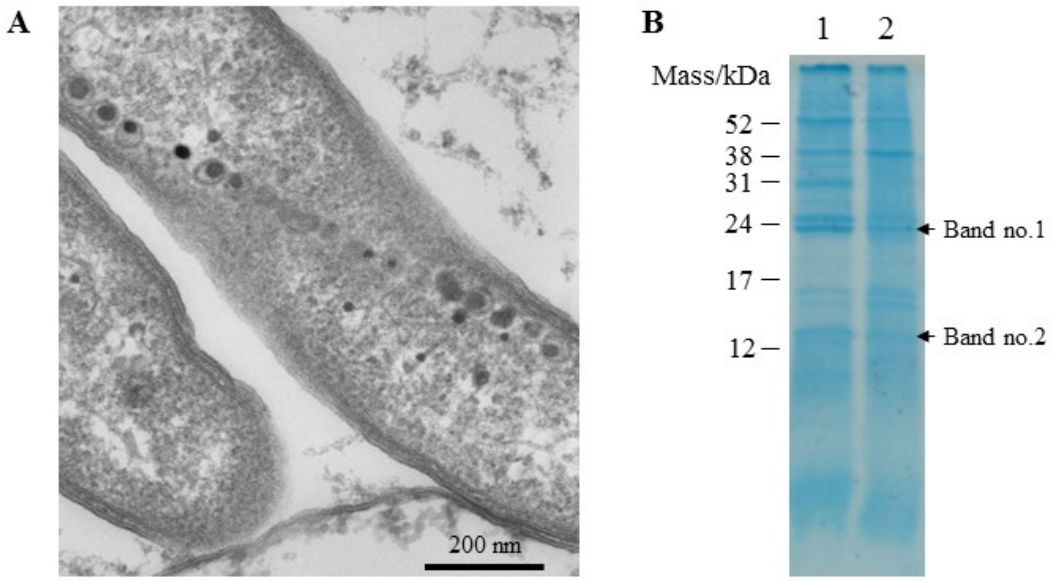

Fig. 3

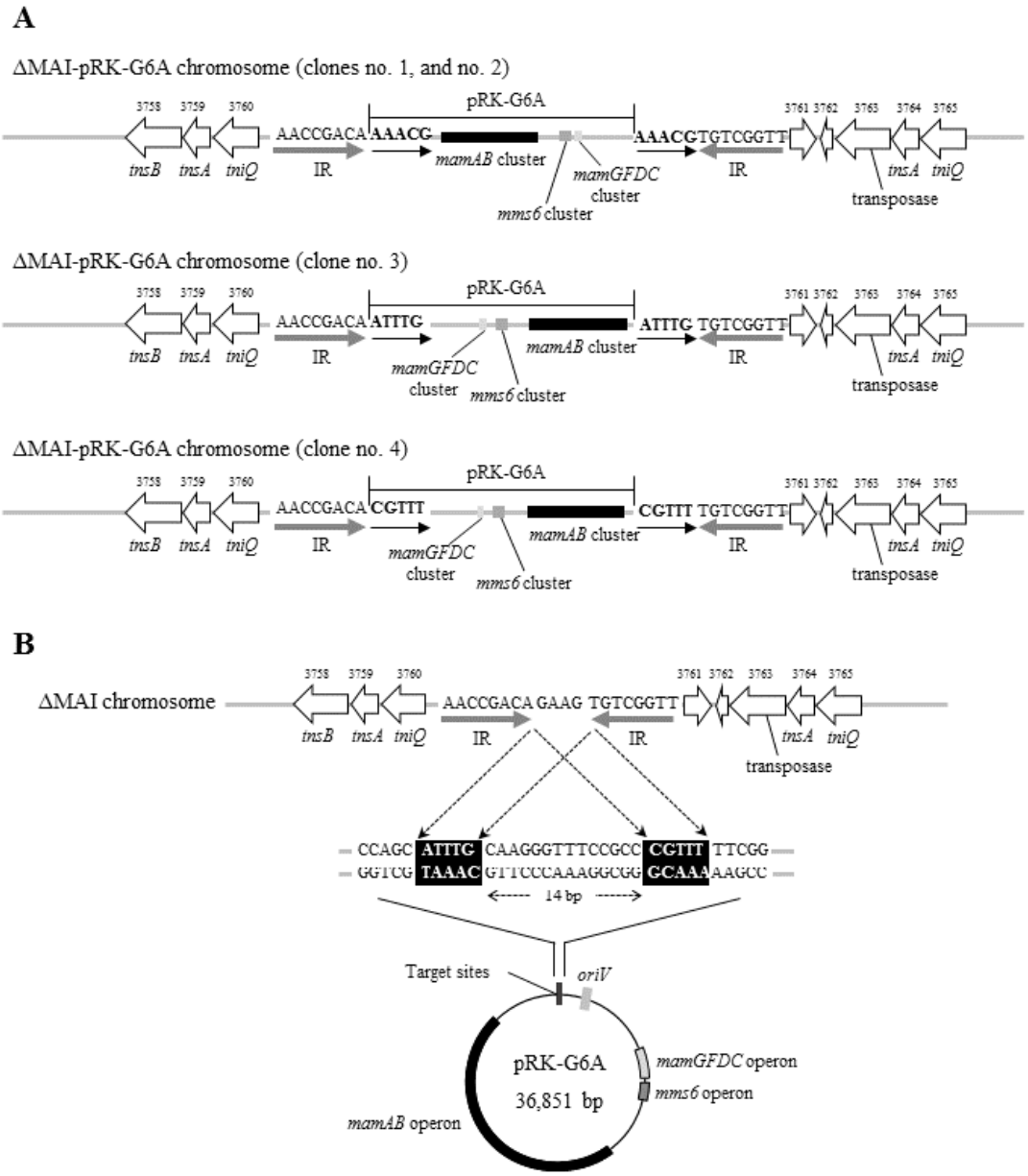
A
ΔMAI-pRK-G6A chromosome (clones no. 1, and no. 2)
pRK-G6A
3758 3759 3760
tnsB tnsA tniQ
AACCGACA AAACG
IR
mamAB cluster
mamGFDC cluster
mms6 cluster
AAACG TGTCGGTT
IR
3761 3762 3763 3764 3765
tnsA tniQ
transposase
ΔMAI-pRK-G6A chromosome (clone no. 3)
AACCGACA ATTTG
ATTTG TGTCGGTT
ΔMAI-pRK-G6A chromosome (clone no. 4)
AACCGACA CGTTT
CGTTT TGTCGGTT
B
ΔMAI chromosome
AACCGACA GAAG TGTCGGTT
CCAGC ATTTG CAAGGGTTTCCGCC CGTTT TTCGG
GGTCG TAAAC GTTCCCAAAGGCGG GCAAA AAGCC
14 bp
Target sites
oriV
pRK-G6A
36,851 bp
mamGFDC operon
mms6 operon
mamAB operon

Fig. 4

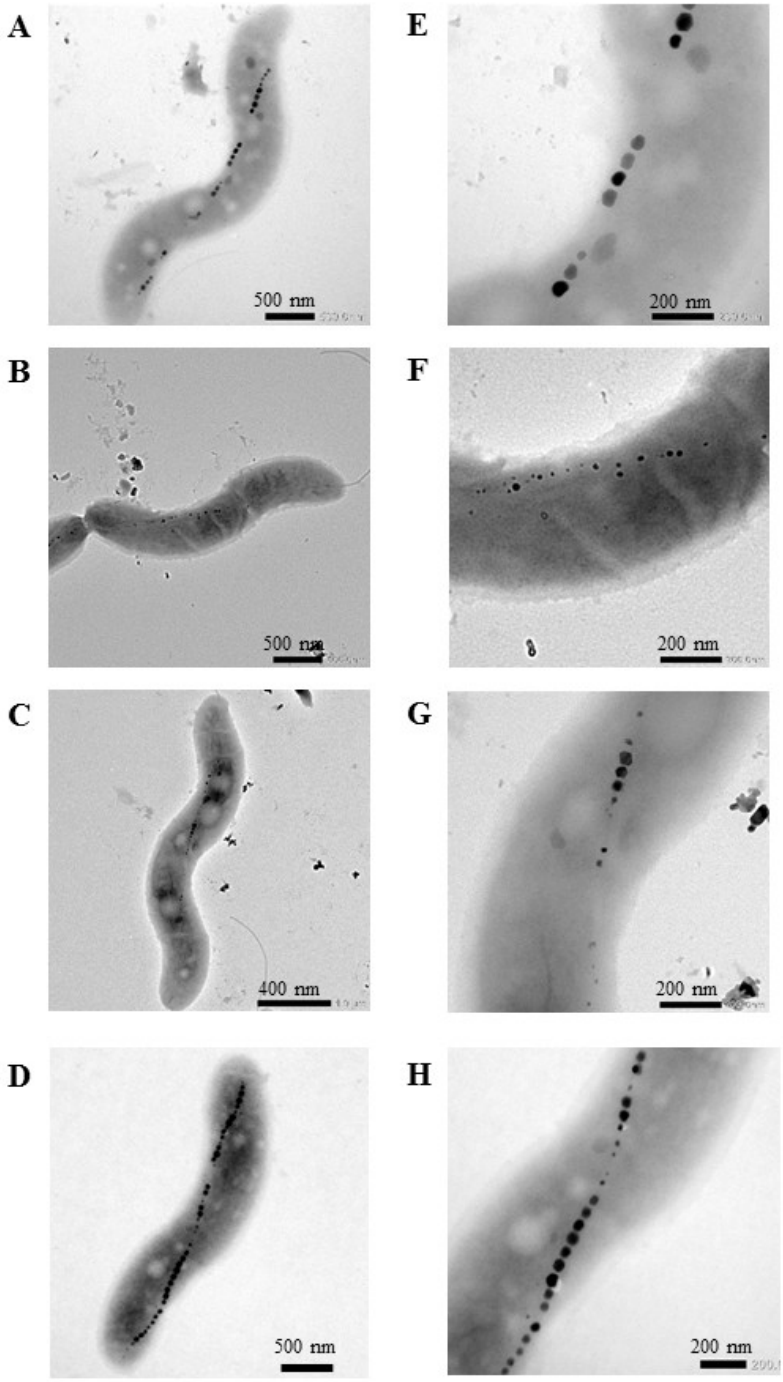

Fig. 5

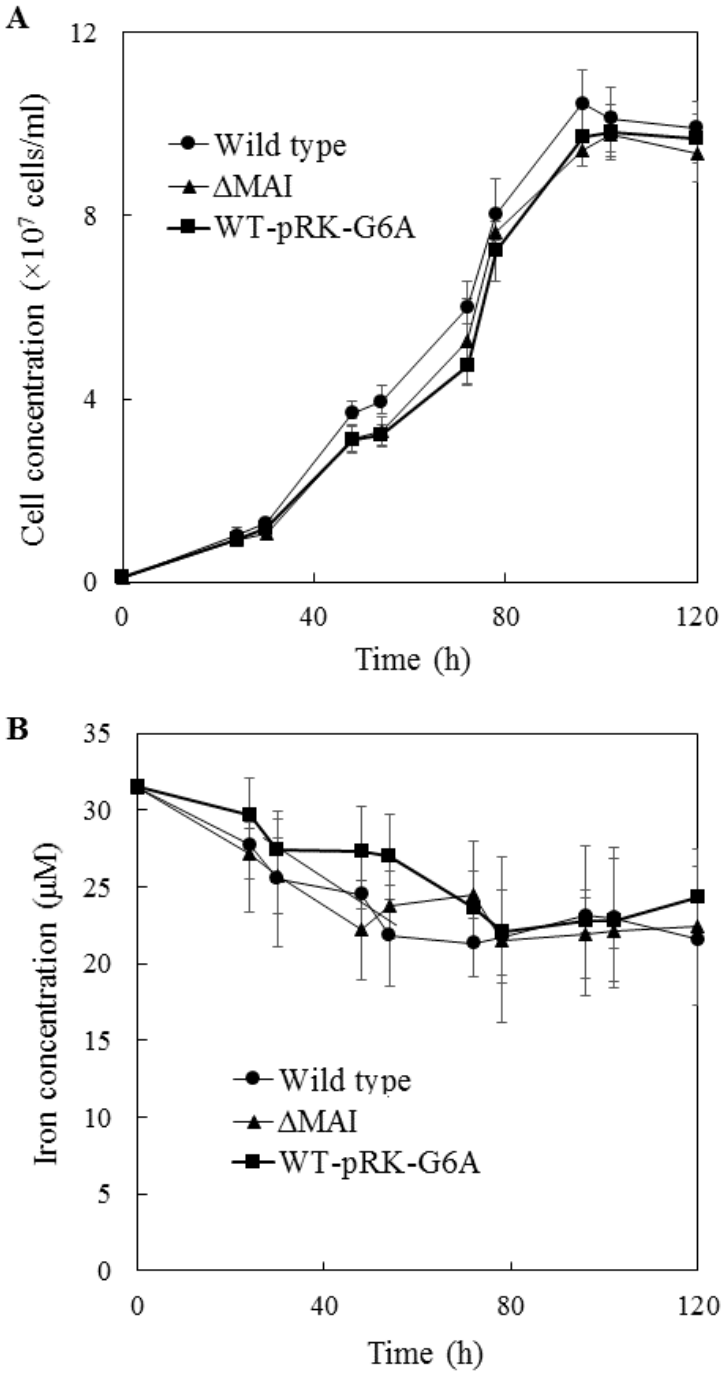
A
12
8
4
0
Cell concentration (×10^7 cells/ml)
Wild type
ΔMAI
WT-pRK-G6A
0
40
80
120
Time (h)
B
35
30
25
20
15
10
5
0
Iron concentration (μM)
Wild type
ΔMAI
WT-pRK-G6A
0
40
80
120
Time (h)

Fig. 6